GEOPHYSICAL RESEARCH LETTERS, VOL. 27, NO. 19, PAGES 3037-3040, OCTOBER 1, 2000

Near-field modeling of the July 17, 1998 tsunami in Papua New Guinea

Philippe Heinrich and Alessio Piatanesi[1]

Laboratoire de Détection et de Géophysique, Commissariat à l'Energie Atomique, Bruyères-le-Châtel, France

Emile Okal

Department of Geological Sciences, Northwestern University, Evanston, IL

Hélène Hébert

Laboratoire de Détection et de Géophysique, Commissariat à l'Energie Atomique, Bruyères-le-Châtel, France

Abstract. Modest earthquakes may trigger large submarine landslides, responsible for disastrous tsunami waves, as demonstrated by the Papua New Guinea event of July 17, 1998. The relatively small earthquake was followed by unexpectedly high waves, up to 15 m, wiping out 3 villages and killing more than 2200 people. Numerical simulations show that seismic dislocation sources are not energetic enough to reproduce the observed tsunami along the coast. Tsunami generation by a submarine landslide has been simulated by a finite-difference model, assimilating the landslide to a flow of granular material. Long-wave approximation is adopted for both water waves and the slide. Numerical results show that observed inundation heights are well reproduced for a volume of 4 km^3 located 20 km offshore, sliding downslope with a Coulomb-type friction.

Introduction

On July 17, 1998, a tsunami devastated the coastline of northern Papua New Guinea (PNG) [*Tappin et al.*, 1999; *Kawata et al.*, 1999; *Piatanesi and Heinrich*, 2000], with run-up heights reaching as much as 15 m at a location on the Eastern spit of Sissano Lagoon (Fig. 1). This tsunami is unusual in at least two respects: first, the discrepancy between run-up amplitudes and the relative moderate size of the parent earthquake (M_s = 6.9 and a value of only 3.7 $\times 10^{19}$ N-m for the final estimate of its seismic moment) [*Tanioka*, 1999]; in addition, it features an extreme concentration of the wave energy on a narrow stretch of coastline: as documented by 80 inundation heights measured along a 40-km section of coast during a post-tsunami survey, run-up heights greater than 7 m were restricted to a 20-km coastal segment, centered at Sissano Lagoon (Fig. 2). Outside this segment, they decrease very rapidly, both eastwards and westwards to benign values of 2 m or less. Both properties are unusual, even considering the so-called "tsunami earthquakes" [*Kanamori*, 1972], whose tsunamis are greater than expected from their seismic waves. Based on Newman and Okal's E/M_0 discriminant [*Newman and Okal*, 1998], the PNG earthquake did not possess the slow source characteristic of tsunami earthquakes such as the 1992 Nicaragua, 1994 Java, or 1996 Peru events [*Imamura et al.*, 1993; *Heinrich et al.*, 1998]. Similarly, in most recent tsunamis, comparable run-up heights were spread over a much longer (100 km) segment of coast.

It should be noted that, inside the coastal segment most inundated, strong variations of the measured run-up heights are observed, probably linked to changes in vegetation density. From these variations, it can be inferred that the highest run-up values are reached close to the shoreline in areas with dense vegetation, against which tsunami waves either break or are reflected.

Seismic Sources

We first consider seismic dislocation sources as the mechanism of generation of the tsunami. The CMT focal solution of the mainshock (Fig. 1) can be interpreted along either fault plane: a classic low-angle thrust subduction with the epicenter (determined by USGS) located on the coast; or the conjugate mechanism, a compressional event on a steep reverse fault. It is unlikely that rupture along the high-angle reverse fault plane could explain the tsunami for several reasons: it would have generated larger coseismic displacements, possibly a fault break, in the immediate vicinity of the epicenter, i.e., on land near Serrano, which were not observed; the distribution of widely scattered aftershocks (whose depth resolution is very poor) is generally more consistent with the low-angle thrust fault geometry; finally, the azimuthal disparity between the strike of faulting and the direction of rupture [*Kikuchi et al.*, 1998] would require significant down-dip propagation of the rupture, which would hamper tsunami generation. Nevertheless, we consider both geometries and compute the co-seismic vertical displacement field induced by fault rupture, using the analytical formalism of Mansinha and Smylie [1971] adapted to the case of a fault rupturing at an angle from the strike direction. This point has been ignored in previous studies, e.g., Matsuyama et al. [1999], who have used the 2nd source to model the effect of small-scale bathymetry on the amplification of the tsunami waves. The resulting field is then taken as the initial field for the hydrodynamic computation.

[1]Now at Dipartimento di Fisica, Settore di Geofisica, Università di Bologna, Bologna, Italy.

Paper number 2000GL011497.
0094-8276/00/2000GL011497$05.00

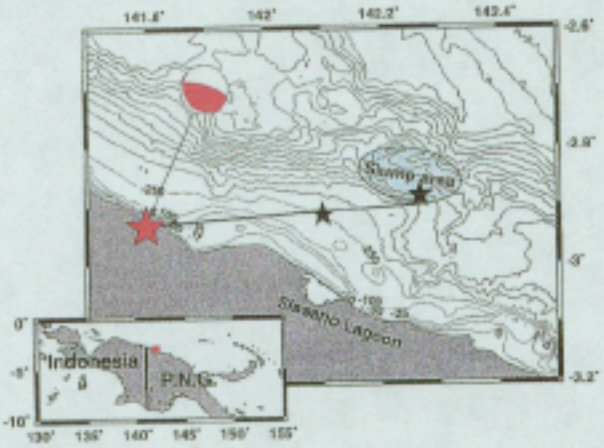

Figure 1. Bathymetric map of northern Papua New Guinea. The stars indicate the epicenter locations of the main shock at 08:49 GMT (in red) and of a large aftershock doublet at 09:09 and 09:10 GMT (in black). The solid line joining them is the horizontal extent of the seismic rupture, as used in the dislocation model. The slump area detected by the marine survey is indicated by the shaded ellipse. The interval of isobaths is 250 m.

Description of the Tsunami Model

Tsunami propagation is modeled in an area of 80 × 80 km^2, using the classic shallow water assumption, since frequency dispersion plays a minor role for short propagation distances. The nonlinear long wave equations are solved by means of a staggered-grid finite-difference method. The numerical model uses a Godunov-type scheme, extended to second order by using the concept of Vanleer [*Mangeney et al.*, 2000; *Alcrudo et al.*, 1993], it is particularly adapted to propagate strongly nonlinear waves. The model, with a grid step of 100 m, cannot take into account the vegetation density so that final run-up is not calculated; rather, the computation is stopped at the flow depth on the shoreline, the latter being taken as a perfect reflector, which is the most realistic way of modeling the largest observed heights with a grid step of 100 m. Our model, referred to in the literature as a threshold-type model [*Titov et al.*, 1998], uses a minimum depth contour of 5 m.

Numerical Results for Seismic Sources

For both seismic sources, the maximum calculated water heights strongly underestimate the measured values (Fig. 2). In order to reproduce the observed values quantitatively, an amplification factor of 12 (1st mechanism) or 80 (2nd mechanism) has to be applied to the profiles shown on Figure 2. In turn, this would lead to increasing the slip on the dislocation by a similar factor, which is inconsistent with the seismic moment of the earthquake. Note the strong deficiency in amplitude for the 2nd source, which reflects the downward extension of the source, necessary to reconcile the epicenter geometry, the direction of propagation, the dip of the fault, and the location of the aftershocks. This argument, in favor of a large submarine landslide as a tsunamigenic source, is supported by the following observations:

- Most reliable witnesses report the tsunami attack immediately following the main aftershock, *i.e.* 20 to 22 minutes after the mainshock, whereas the travel time of water waves is only about 10 minutes from a source located 20 km offshore away from Sissano (an aftershock did take place at 09:02 GMT, 13 minutes after the mainshock, but it is much too small, m_b = 4.4, for its dislocation to be the tsunami source). The 10-minutes hiatus could be accounted for by a time delay between the mainshock and the triggering of the sediment slump.
- Several water waves were observed along the coast, the first one not always being the largest, which is not obtained using the proposed seismic sources.
- Bathymetric and seismic reflection surveys have detected, in an amphitheater-shaped depression of 50 km^2 (Fig. 1), the internal structure of a rotational slump with an estimated volume of 4 km^3 and a few hundred meters thick, that has slid a few kilometers away from its presumed initial position [*Tappin et al.*, 1999].
- *T* waves generated by the 09:02 aftershock were recorded at Wake Island [*Okal et al.*, 1999], lasting close to one minute, an abnormally long duration for a seismic shock with m_b = 4.4, suggesting that the 09:02 event may be a landslide rather than a seismic dislocation.

Description of the Landslide Model

Modeling a landslide is then required. The volume of the landslide is taken as 4 km^3, located in the above-mentioned depression (Fig. 3). The mechanism initiating the landslide is not studied and it is assumed that the whole mass suddenly loses its equilibrium and slides downslope under gravity forces. The landslide is treated as a fluid-like flow of a cohesionless granular material. Interfacial mixing with water is assumed to be negligible due to the short run-out distance and the interfacial shear is assumed to be small compared to the basal friction [*Jiang and LeBlond*, 1992; *Rabinovich et al.*, 1999]. Since the slide thickness is much smaller than the characteristic slide length, mass and momentum conservation equations are depth-averaged over the thickness in a way similar to tsunami equations, which allows to ignore the precise mechanical behavior within the flow [*Savage and Hutter*, 1989]. The deformation is assumed to be essentially

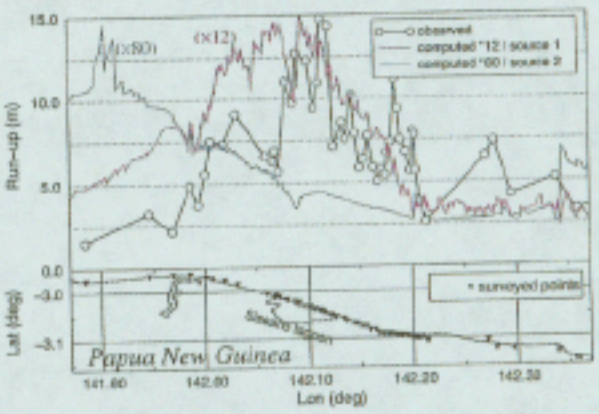

Figure 2. Comparison between observed run-up heights (open circles) and maximum calculated water heights for the two seismic dislocation models considered. For both sources, the fault length is 42 km rupturing at an azimuth of 85° and the slip dislocation is 1m06. The strike, dip and rake angles are for the 1st source (subduction event) 146°, 19° and 127° and for the 2nd source (steep reverse fault) 287°, 75°, 78°.

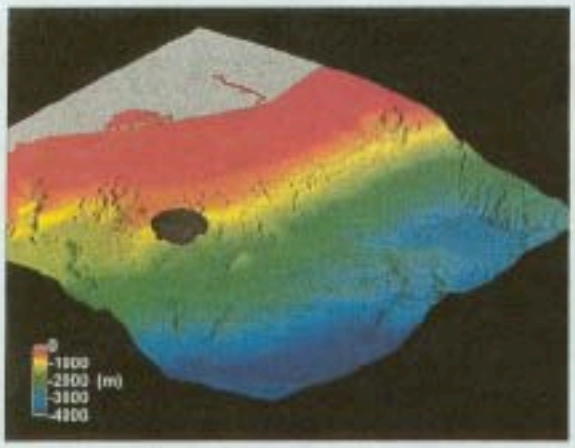

Figure 3. 3-D view of the bathymetry and of the landslide (in black). The landslide volume, defined as the intersection of an ellipsoid with the existing bathymetry, covers an area of about 5 by 3 km, with a maximum thickness of 450 m. It is located at water depths between 550 and 1500 m, on a 15° slope. The horizontal dimensions of the domain are 55×55 km.

located in a thin boundary layer near the bed surface, as often observed in landslide deposits where pre-failure stratigraphy is preserved. Energy dissipation is then neglected within the flow and is limited to basal friction modeled by a Coulomb-type friction law. This law assumes a constant ratio of the shear stress to the normal stress at the base and involves a dynamic friction angle φ between the rough bed and the mass. When the flow is close to rest, the fluid velocity is set to 0 as soon as the Coulomb force is larger than the algebraic sum of the forces due to gravity and height gradient. This approach, which allows the flow to stop, is more appropriate to debris avalanches than to slumps, composed of cohesive rocky material. Other approaches could be tested in the early stages of the collapse, the analytical model of Watts [1998] considering a solid block motion or the numerical model of Tinti et al. [1999] who consider the landslide as a rigid body structured in blocks interacting with each other. The resulting equations of mass and momentum conservation, written in a coordinate system linked to the topography, read :

$$\frac{\partial h}{\partial t}+\frac{\partial}{\partial x}(hu)+\frac{\partial}{\partial y}(hv)=0 \qquad (1)$$

$$\frac{\partial}{\partial t}(hu)+\frac{\partial}{\partial x}(hu.u)+\frac{\partial}{\partial y}(hu.v)= -\frac{1}{2}\kappa\frac{\partial}{\partial x}(gh^2\cos\theta)+\kappa gh\sin\theta_x+F \qquad (2)$$

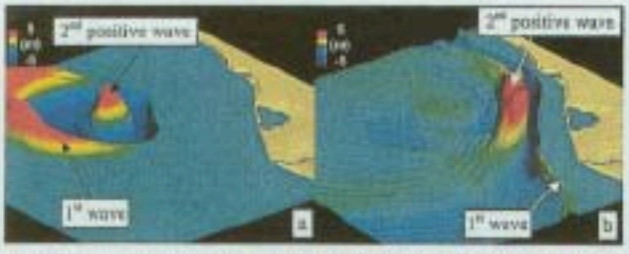

Figure 4. Snapshots of the computed water surface at $t=90$ s *(a)* and $t=360$ s *(b)* after the slide initiation. Same horizontal dimensions as in Fig. 3. Vertical scale is exaggerated by a factor 750 with respect to horizontal scale.

$$\frac{\partial}{\partial t}(hv)+\frac{\partial}{\partial x}(hv.u)+\frac{\partial}{\partial y}(hv.v)= -\frac{1}{2}\kappa\frac{\partial}{\partial y}(gh^2\cos\theta)+\kappa gh\sin\theta_y+F_y \qquad (3)$$

where $\kappa=1-\rho_e/\rho_s$, $F=-\kappa\, gh\cos\theta\tan\varphi\, u/|u|$ is the friction force, $u=(u,v)$ is the depth-averaged velocity vector parallel to the bed, h is the slide thickness perpendicular to the slope, ρ_e and ρ_s are the water and sediments densities with a ratio $\rho_e/\rho_s=2$, $\theta(x,y)$ is the local steepest slope angle, θ_x and θ_y are the slope angles along x- and y-axis respectively. These hyperbolic equations are solved by the same numerical scheme as the one used in the tsunami model.

The associated water waves are calculated by solving shallow water equations. Sea-bottom time deformation induced by the landslide passage is introduced as a known forcing term $(\cos\theta)^{-1}\partial h/\partial t$ in the mass conservation equation of the tsunami model. This term is appropriate in a shallow water context, when the horizontal scale of the disturbance is large compared to the water depth [*Tinti et al.*, 1999].

Simulation of a Landslide-Generated Tsunami

At the source location, three major waves are produced by the landslide [*Rzadkiewicz et al.*, 1997]. The water ahead of the front face of the slide is pushed away, creating a leading positive wave in the slide direction. The second wave is a large trough simultaneously created by the slide aspiration, and is followed by a large second positive wave created by the filling-in of the trough (Fig. 4). The three waves spread outward from the source as cylindrical waves. The 20-km stretch centered at Sissano lagoon entrance is affected only by the second positive wave, preceded by the trough (Fig. 4). It is worth noting that this wave does not spread out laterally (Fig. 1), due to energy focusing by a shallow shelf that extends offshore for 10 km from Sissano region [*Matsuyama et al.*, 1999]. Beyond this coastal segment, the coast is reached by the first positive wave, with reduced amplitude due to geometric dispersion. It is followed by the trough and later by the second positive wave.

As expected, numerical tests show that water wave amplitudes are considerably reduced for the same volume when increasing the mean depth of the landslide. It is also

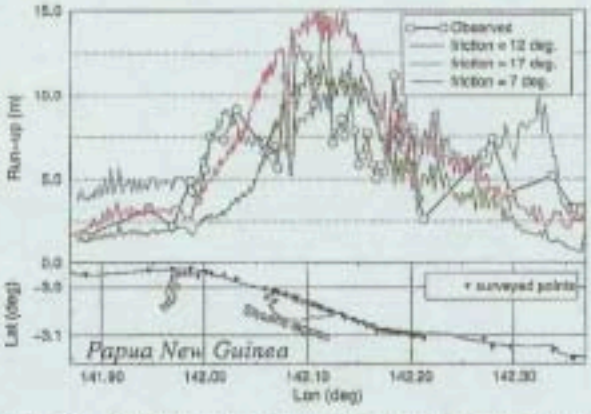

Figure 5. Comparison between observed run-up heights (open circles) and maximum heights of water waves generated by a landslide with a volume of 4 km^3. Numerical tests for 3 friction angles $\varphi=7°$ (blue), $\varphi=12°$ (red) and $\varphi=17°$ (green).

shown that the maximum inundation heights depend weakly on the landslide lateral position within the depression. Surprisingly, one major parameter controlling the run-up distribution is the friction law governing the landslide. Sensitivity tests were carried out by varying the basal friction angle φ, in the range determined by back-calculations from datasets of subaerial rock avalanches [*Voight*, 1979], *i.e.* from 5° to 20°. Numerical results show that the calculated distribution is flatter than the observed one for small friction angles (Fig. 5). The smaller the friction angle, the higher the slide velocity, which produces in the generation area a larger first positive wave, that remains higher when reaching the coast outside Sissano. On the opposite, the 2nd positive wave is attenuated in the generation area and later in Sissano region. This attenuation is accounted for by a longer duration of the landslide, so that water aspiration by the slide interferes with the filling-in of the trough. The best fit to observations is obtained for φ=12°, considering that the calculated water waves are reflected waves against the shoreline. In this case, the emplacement time for the leading edge of the landslide is slightly less than 2 minutes, the maximum vertical fall is about 500 m for a run-out distance of about 5 km. This distance, close to the observed one, is reduced to 2 km for φ=17° and exceeds 20 km for friction angles lower than 7°.

Conclusion

The analysis of the 1998 Papua New Guinea event by means of numerical simulations confirms the large submarine landslide as the most probable origin of the tsunami. In other instances (Flores, 1992; Okushiri, 1993), local amplification of run-up has been attributed to localized underwater landslides of contained dimensions, triggered by the earthquake. This case differs in the much larger scale of the phenomenon, as well as in its nature as a slump. An important lesson learned from the PNG event is that catastrophic slides can be triggered by relatively moderate earthquakes, in the present case with a moment well below 10^{20} N-m, a figure heretofore often quoted as a threshold for regional tsunami hazard.

Acknowledgments. The authors are grateful to O. Pouliquen (IUSTI, Marseille University) for fruitful discussions concerning the friction law, and to D. Tappin, Ph. Watts and SOPAC Institute for providing bathymetric data and estimates of the slide geometry.

References

Alcrudo, F., and P. Garcia-Navarro, A high-resolution Godunov-type scheme in finite volumes for the 2D shallow water equations, *Int. J. for Num. Meth. in Fluids, 16*, 489-505, 1993.

Heinrich, Ph. *et al.*, Modeling of the February 1996 Peruvian tsunami, *Geophys. Res. Lett., 25*, 2687-2690, 1998.

Imamura, F. *et al.*, Estimate of the tsunami source of the 1992 Nicaraguan earthquake from tsunami data, *Geophys. Res. Lett., 20*, 1515-1518, 1993.

Jiang, L., and P. LeBlond, The coupling of a submarine slide and the surface waves it generates, *J. Geophys. Res., 97*, 731-744, 1992.

Kanamori, H., Mechanism of tsunami earthquakes, *Phys. Earth Planet. Inter. 6*, 346-359, 1972.

Kawata, Y. *et al.*, Tsunami in Papua New Guinea was as intense as first thought, *Eos Trans. AGU, 80*, 101, 104-105, 1999.

Kikuchi, M. *et al.*, Source rupture process of the Papua New Guinea Earthquake of July 17, 1998 inferred from teleseismic body waves, *Eos Trans. AGU, 79*, (45), abstract, 1998.

Mangeney, A., Heinrich, Ph., and R. Roche, Analytical and numerical solution of dam-break problem for application to water floods, debris and dense snow avalanche, *Pure Appl. Geophys., 157*, in press, 2000.

Mansinha, L., and D. Smylie, The displacement fields of inclined faults, *Bull Seismol. Soc. Amer., 61*, 1433-1440, 1971.

Matsuyama, M., Walsh, J., and H. Yeh, The effect of bathymetry on tsunami characteristics at Sissano lagoon, Papua New Guinea, *Geophys. Res. Lett., 26*, 3513-3516, 1999.

Newman, A., and E. Okal, Teleseismic estimates of radiated seismic energy: the E/M_0 discriminant for tsunami earthquakes, *J. Geophys. Res., 103*, 26885-26898, 1998.

Okal, E., The probable source of the 1998 Papua New Guinea tsunami as expressed in oceanic T waves (abstract), *Eos Trans. AGU, 80*, 46, 1999.

Piatanesi, A., and Ph. Heinrich, Source characteristics of the July 17 Papua New Guinea tsunami inferred from run-up data, *J. Geophys. Res.*, submitted, 2000.

Rabinovich et al., The landslide-generated tsunami of November 3, 1994 in Skagway harbor, Alaska, a case study, *Geophys. Res. Lett., 26*, 3009-3012, 1999.

Rzadkiewicz, S., Mariotti, C., and Ph. Heinrich, Numerical simulation of submarine landslides and their hydraulic effects, *J. of Wtrways, Port, Coast., and Oc. Engnrg., 123*, 149-157, 1997.

Savage, S., and K. Hutter, The motion of a finite mass of granular material down a rough incline, *J. Fluid Mech., 199*, 177-215, 1989.

Tanioka, Y., Analysis of the far-field tsunamis generated by the 1998 Papua New Guinea earthquake, *Geophys. Res. Lett., 26*, 3393-3396, 1999.

Tappin, D. *et al.*, Sediment slump likely caused 1998 Papua New Guinea tsunami, *EOS, 80*, 329, 334, 340, 1999.

Tinti, S., Bortolucci, E. and A. Armigliato, Numerical simulation of the landslide-induced tsunami of 1988 in Vulcano island, Italy, *Bull. Volcanol.*, 61, 121-137, 1999.

Titov, V., and C. Synolakis, Numerical modeling of tidal wave runup, *J. of Wtrways, Port, Coast., and Oc. Engnrg., 124*, 157-170, 1998.

Voight, B., *Rockslides and avalanches, 2, Engineering Sites.* (B. Voight, ed.), Developments in Geotechnical Engineering, Vol. 14B, Elsevier Scientific Publishing Company, 1979.

Watts, P., Wavemaker curves for tsunamis generated by underwater landslides, *J. of Wtrways, Port, Coast., and Oc. Engrg., 124*, 127-137, 1998.

H. Hébert, P. Heinrich, A. Piatanesi, LDG/CEA, B.P. 12, 91680 Bruyères-le-Châtel, France. (e-mail: heinrich@ldg.bruyeres.cea.fr)

E. Okal, Department of Geological Sciences, Northwestern University, Evanston, IL 60208 (e-mail: emile@earth.nwu.edu)

(Received February 14, 2000; accepted May 19, 2000)